Molecular Biology of the Cell
Vol. 17, 3291–3303, July 2006

Rho Kinase, Myosin-II, and p42/44 MAPK Control Extracellular Matrix-mediated Apical Bile Canalicular Lumen Morphogenesis in HepG2 Cells[D] [V]

Hilde Herrema,* Dominika Czajkowska,* Delphine Théard,* Johanna M. van der Wouden,* Dharamdajal Kalicharan,† Behnam Zolghadr,* Dick Hoekstra,* and Sven C.D. van IJzendoorn*

Sections of *Membrane Cell Biology and †Electron Microscopy, Department of Cell Biology, University Medical Center Groningen, University of Groningen, 9713 AV Groningen, The Netherlands

Submitted January 24, 2006; Revised April 18, 2006; Accepted April 27, 2006
Monitoring Editor: Keith Mostov

The molecular mechanisms that regulate multicellular architecture and the development of extended apical bile canalicular lumens in hepatocytes are poorly understood. Here, we show that hepatic HepG2 cells cultured on glass coverslips first develop intercellular apical lumens typically formed by a pair of cells. Prolonged cell culture results in extensive organizational changes, including cell clustering, multilayering, and apical lumen morphogenesis. The latter includes the development of large acinar structures and subsequent elongated canalicular lumens that span multiple cells. These morphological changes closely resemble the early organizational pattern during development, regeneration, and neoplasia of the liver and are rapidly induced when cells are cultured on predeposited extracellular matrix (ECM). Inhibition of Rho kinase or its target myosin-II ATPase in cells cultured on glass coverslips mimics the morphogenic response to ECM. Consistently, stimulation of Rho kinase and subsequent myosin-II ATPase activity by lipoxygenase-controlled eicosatetranoic acid metabolism inhibits ECM-mediated cell multilayering and apical lumen morphogenesis but not initial apical lumen formation. Furthermore, apical lumen remodeling but not cell multilayering requires basal p42/44 MAPK activity. Together, the data suggest a role for hepatocyte-derived ECM in the spatial organization of hepatocytes and apical lumen morphogenesis and identify Rho kinase, myosin-II, and MAPK as potentially important players in different aspects of bile canalicular lumen morphogenesis.

INTRODUCTION

Hepatocytes develop from hepatoblasts and adopt a specific polarized architecture and therewith correlated functions in response to proper environmental cues (reviewed in Kinoshita and Miyajima, 2002; Lemaigre and Zaret, 2004; Zhao and Duncan, 2005). In vivo, fetal hepatocytes develop in cords that are three to five cells thick, which are reduced to one- or two-cell–thick cords in mature hepatocytes. In the cords, each hepatocyte is attached to its neighbors in a two-dimensional plate. On either side of the cord, each hepatocyte faces the space of Disse, across which it communicates freely with adjacent blood-filled sinusoids. In contrast to simple epithelial cells, which sit on their basal surface and have an apical surface exposed to the external space while attached to their neighbors along the lateral surface, hepatocytes display a unique topology (Figure 1). Thus, a typical hepatocyte displays two basal surfaces on opposite ends of the cell where it faces the sinusoids on either side of the cord in which it resides (reviewed in Stamatoglou and Hughes, 1994). A portion of the lateral domain of hepatocytes is modified to form the apical surfaces that line the bile canaliculi, which in vivo form an intercellular network of narrow passages contained within each cord. The bile canaliculi are thought to develop from small vacuoles between adjacent hepatocytes before bile formation starts, consistent with the existence of functional mechanisms for sorting of plasma membrane molecules early in development (Feracci *et al.*, 1987). In the primordial stage, the small vacuoles give rise to extended bile canaliculi that line several hepatocytes. Functional bile canalicular lumens are separated from the perihepatocytic space by the presence of tight junctions and desmosomes.

An early step in the development of canalicular lumens is the biogenesis of apical plasma membranes to accommodate bile canalicular functions. Studies with primary hepatocyte cultures and hepatic cell lines have revealed several processes that contribute to apical plasma membrane biogenesis and the development of intercellular apical vacuoles (reviewed in Zegers and Hoekstra, 1997; Gallin, 1997; Wang and Boyer, 2004). Signaling cascades induced by interleukin-6 family cytokines such as oncostatin M stimulate fetal

This article was published online ahead of print in *MBC in Press* (http://www.molbiolcell.org/cgi/doi/10.1091/mbc.E06–01–0067) on May 10, 2006.

[D] [V] The online version of this article contains supplemental material at *MBC Online* (http://www.molbiolcell.org).

Address correspondence to: Sven C.D. van IJzendoorn (s.c.d.van.ijzendoorn@med.umcg.nl).

Abbreviations used: BC, bile canalicula(i); BDM, 2,3-butanedione; BSA, bovine serum albumin; C6-NBD, 6-[*N*-(7-nitrobenz-2-oxa-1,3-diazol-4-yl)amino]hexanoic acid; ECM, extracellular matrix; ETA, eicosatetranoic acid; FCS, fetal calf serum; HBSS, Hank's balanced salt solution; MLC2, myosin light chain 2; NDGA, nordihydrouaiaretic acid; R123, rhodamine 123; ROCK, rho kinase; SM, sphingomyelin; TEM, transmission electron microscopy.

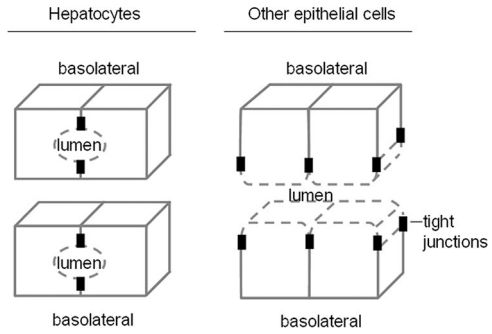

Figure 1. Schematic drawing that shows the orientation of the apical lumen shared by a pair or a group of hepatocytes (left side) in comparison with other epithelial cells such as those found in the kidney or intestine (right side). Dotted and solid lines represent the apical and basolateral surfaces, respectively.

liver development, establishment of intercellular contacts, and the formation of apical plasma membranes (Matsui *et al*., 2002; van der Wouden *et al*., 2002). Oncostatin M-stimulated apical plasma membrane biogenesis requires protein kinase A, which has been implicated in apical surface-directed membrane trafficking (van IJzendoorn *et al*., 1997; Zegers and Hoekstra, 1998; Roelofsen *et al*., 1998; van IJzendoorn and Hoekstra, 1998), and, in this way, regulate the supply of specific proteins and lipids from subapical recycling endosomes to the developing apical surface (reviewed in van IJzendoorn and Hoekstra, 1999; Hoekstra *et al*., 2004). Furthermore, the regulated exchange of proteins and lipids between the endosomal system and developing apical surface is tightly controlled by dihydroceramide synthase-regulated sphinganine metabolism (van IJzendoorn *et al*., 2004b); the cell cycle regulatory proteins $p27^{Kip1}$ and cyclin-dependent kinase 2 (van IJzendoorn *et al*., 2004a); and small GTPase rab proteins, including rab11 (Wakabayashi *et al*., 2005) and rab3d (Larkin *et al*., 2000). Although these and other studies have revealed some of the molecular mechanisms that control the biogenesis of apical plasma membrane domains in hepatocytes, and, in this way, the early steps in the formation of intercellular vacuoles with compositional and functional characteristics of bile canaliculi, polarizing hepatic cell lines (e.g., HepG2 or WIF-B; Ihrke *et al*., 1993), and primary hepatocytes in culture do not typically form subsequent elongated canalicular networks as observed in vivo. Consequently, virtually nothing is known about the molecular mechanisms that control the formation of multicellular apical canaliculi.

The spatial organization and polarized architecture of hepatocytes is likely to be dictated by interaction of the cells with the extracellular environment, e.g., neighboring cells and the extracellular matrix (ECM; reviewed in Stamatoglou and Hughes, 1994). The space of Disse contains most major ECM molecules, the majority of which are derived from endothelial cells and hepatic stellate (Ito) cells (Friedman *et al*., 1985; Senoo *et al*., 1998). In addition, hepatocytes produce ECM (Selden *et al*., 2000), albeit at significantly lower quantities. Some isolated ECM components have been reported to induce transcription of a subset of liver-specific genes (DiPersio *et al*., 1991) and to facilitate the formation of extended apical canaliculi in hepatocytes cultured either in suspension (Tzanakakis *et al*., 2001; Abu-Absi *et al*., 2002) or in an ECM "sandwich" configuration (Berthiaume *et al*., 1996; Moghe *et al*., 1996). It is not clear, however, whether hepatocyte-derived ECM contributes to hepatocytic morphogenic processes, and, importantly, which molecular mechanisms and signaling pathways are involved in bile canalicular lumen morphogenesis.

The aim of this study was to find culture conditions and molecular parameters that promote the development of multicellular canalicular lumens. It is demonstrated that human hepatic HepG2 cells cultured on coverslips first develop intercellular apical vacuoles between two or three neighboring cells. On the deposition of HepG2 cell-derived ECM molecules, however, the cells display clustering, multilayering, and a dramatic remodeling of the apical vacuoles resulting in the development of extended apical lumens that span multiple cells, and resemble the organizational pattern during development, regeneration, and neoplasia of the liver. Our data indicate a critical role for Rho kinase and myosin-II ATPase activity as well as a requirement for p42/44 MAPK signaling in cellular reorganization and/or apical lumen morphogenesis mediated by hepatocyte-derived ECM.

MATERIALS AND METHODS

DMEM and Hank's balanced salt solution (HBSS) were from Invitrogen (Carlsbad, CA). Y-27632 was obtained from Calbiochem (San Diego, CA). Eicosa-5*Z*,8*Z*,11*Z*,14*Z*-tetraenoic acid (eicosatetranoic acid; ETA), nordihydroguaiaretic acid (NDGA), and 2,3-butanedione monoxime (BDM) were purchased from Sigma-Aldrich (St. Louis, MO). Blebbistatin was obtained from Toronto Research Chemicals (North York, Ontario, Canada). 2′-Amino-3′-methoxyflavone (PD98059) was purchased from LC Laboratories (Woburn, MA). Mouse monoclonal anti-villin and monoclonal anti-ZO-1 antibodies were from Transduction Laboratories (Newington, NH) and Zymed Laboratories (South San Francisco, CA), respectively. Mouse monoclonal antibodies (mAbs) against MLC2, phospho (ser18/19)-MLC2, p42/44 MAPK, and phospho-p42/44 MAPK were from Cell Signaling Technology (Beverly, MA). A mouse mAb against MRP2 (M2 III-6) was obtained from Abcam (Cambridge, MA), and a polyclonal antibody raised against fibronectin was purchased from Chemicon International (Temecula, CA). Alexa-488– or Alexa-596–conjugated secondary antibodies and 6-[*N*-(7-nitrobenz-2-oxa-1,3-diazol-4-yl) amino]hexanoic acid (C_6-NBD) were purchased from Molecular Probes (Eugene, OR).

Inhibitors

Pharmacological inhibitors were used at concentrations and time intervals reported previously in the literature and/or indicated by the manufacturer: Y-27632, 2.5 μM for 24–72 h, which effectively inhibits phosphorylation of myosin-II by Rho kinase in response to ETA (cf. Figure 7); ETA, 50 μM for 24–72 h, previously shown to stimulate Rho kinase (Araki *et al*., 2001); NDGA, 10 μM, which effectively blocks ETA-induced effects in HepG2 cells (cf. Figure 6); and BDM and blebbistatin, 10 mM and 100 μM, respectively, for 24 h. In control experiments, cells were treated with vehicle only.

Cell Culture

Human HepG2 cells (ATCC HB8065) were cultured in DMEM containing 4500 mg of glucose/l supplemented with 10% heat-inactivated (30 min at 56°C) fetal calf serum (FCS), 2 mM L-glutamine, 100 IU/ml penicillin, and 100 μg/ml streptomycin in a humidified atmosphere (5% CO_2 in air) at 37°C. Media were changed every other day. Cells were grown in 25-cm^2 culture flasks or plated at low density onto ethanol-sterilized glass coverslips for experiments.

ECM Deposition

HepG2 cells were plated on coverslips and cultured until a confluent layer was formed (typically 3–5 d). To remove the cells without affecting the deposited ECM, use of digestive proteinases such as trypsin was avoided. Instead, the cells were incubated with 2 ml of distilled water per coverslip for 45 min at 37°C. Cells were removed from the coverslips by thorough resuspension. The coverslips were then carefully examined under a light microscope to verify that the cells and cellular debris had been removed. The effective removal of cells and cellular debris with this method was also verified by scanning electron microscopy and (immuno)fluorescent labeling of the decellularized coverslips with the DNA stain 4,6-diamidino-2-phenylindole (DAPI) or antibodies against actin and tubulin. No cells or cellular debris (Supplemental Figure S1D versus S1A; S1H versus S1G), DNA (Supplemental Figure S1E versus S1B), or cytoskeleton remnants (our unpublished data) were present on the coverslip after removal of the cells. Importantly, using antibodies against fibronectin (diluted 1:80), it was demonstrated

that ECM remains on the coverslip after removal of the cells (Supplemental Figure S1F). Fibrillar ECM-like structures could occasionally be observed on decellularized coverslips with scanning electron microscopy (Supplemental Figure S1I and S1J). Only coverslips on which cellular remnants could not be detected with light microscopy were used, and they were subsequently incubated with DMEM for 1 h at 37°C to enable reconformation of matrix proteins. HepG2 cells were plated at low density on the ECM for 24, 48, or 72 h.

Determination of Cell Polarity

Cells were fixed in −20°C absolute ethanol for 10 s and rehydrated in HBSS. Cells were double stained with a mixture of the nuclear stain Hoechst-33528 (5 ng/ml) and tetramethylrhodamine isothiocyanate (TRITC)-labeled phalloidin (100 ng/ml) in HBSS for 20 min at room temperature (RT). After washing, coverslips were mounted, and cells were examined using an epifluorescence microscope (Provis AX70; Olympus, New Hyde Park, NY). Using the focus-tuning knob to scan through the sample, cell polarity was determined by counting the number of cells (identified by fluorescently labeled nuclei) participating in a bile canaliculus (BC; identified by dense F-actin staining lining the BC) and expressed as the percentage of apical lumens shared by two, three, four, or more than five cells. Data are represented as the mean ± SD of three independent experiments, carried out in duplicate. About 50 apical lumens per coverslip were examined. To verify that apical lumens were enclosed within cell clusters, serial confocal x-y sections (typically 1 section/0.5 μm) and subsequent x-z reconstructions were prepared using an acusto-optical beam splitter-based confocal microscope (Leica Microsystems, Heidelberg, Germany). Animated serial x-y sections and corresponding projections were exported as AVI-formatted movie clips using Leica confocal software Lite version 2.61.

Immunostaining

For villin staining, cells were fixed and permeabilized with −20°C acetone for 5 min. After washing with HBSS, cells were blocked in HBSS containing 1% bovine serum albumin (BSA) (wt/vol in HBSS; pH 7.2) for 30 min at RT and subsequently incubated with a mouse mAb against the apical protein villin (1:50 dilution in HBSS) for 2 h at RT. Cells were washed to remove primary antibody, followed by incubation with the secondary goat anti-mouse antibody (2 μg/ml) conjugated with Alexa Fluor-488 (Molecular Probes) for 45 min at RT. For staining for the tight junction protein ZO-1, MRP2, or (phospho)-MLC2, cells were fixed in 4% paraformaldehyde (wt/vol in HBSS; pH 7.2). After washing (3 times in HBSS), cells were permeabilized with 0.1% Triton X-100 (wt/vol in HBSS) for 5 min at RT. Cells were washed and blocked with 1% BSA (wt/vol in HBSS; pH 7.4) for 30 min at RT. BSA was removed, and cells were incubated with the mouse mAb anti-ZO-1 (1:100 dilution in HBSS), anti-MRP2 (1:200 dilution in HBSS), or (phospho)-MLC2 (1:100 dilution in HBSS) for 2, 1, and 1 h at RT, respectively. Cells were washed three times with HBSS and incubated with the secondary antibodies (2 μg/ml) conjugated with Alexa Fluor-488 or -596 (diluted 1:400 in HBSS; Molecular Probes) for 45 min at RT. After incubation with the secondary antibody, cells were washed three times with HBSS and mounted.

Membrane Labeling with Fluorescent Lipid

C_6-NBD-sphingomyelin (SM) was dried under N_2 and redissolved in absolute ethanol. The lipid was used at a concentration of 4 μM in HBSS [final ethanol concentration 0.5% (vol/vol)]. Cells were washed three times with cold HBSS and incubated with C_6-NBD-SM for 30 min at 4°C. To remove noninternalized probes, cells were washed three times with 4°C HBSS, and further incubated with HBSS for 30 min 37°C. After a subsequent three washes with 4°C HBSS, cells were incubated with BSA [5% (wt/vol); pH 7.4] in HBSS, two times for 30 min at 4°C (back exchange). Cells were washed three times and examined immediately using an epifluorescence microscope (Provis AX70; Olympus).

Rhodamine 123 (R123) Incubation

Cells were washed three times with 37°C HBSS and incubated with R123 for 30 min at 37°C. R123 is recruited to the apical membrane and pumped into the BC by ATP-binding cassette transporters. After a wash with 37°C HBSS, cells were examined immediately.

Multilayering

Multilayering was expressed as the percentage of total number of cells (identified by fluorescently labeled nuclei) that multilayer calculated by the following equation: multilayering = $((\text{nuclei}_{\text{total}} - \text{nuclei}_{\text{single}})/\text{nuclei}_{\text{total}}) \times 100\%$, in which $\text{nuclei}_{\text{single}}$ refers to nuclei that do not visibly overlap with other nuclei in the x-z direction. At least 10 fields per coverslips, each containing >50 cells, were analyzed.

Western Blotting

Cells were lysed in lysis buffer (10 mM triethanolamine, pH 7.4, 1.0% Triton X-100, 0.1% SDS, 100 mM NaCl, 1 mM EDTA, 1 mM EGTA, 1 mM NaF, 20 mM $Na_4P_2O_7$, and 2 mM sodium vanadate, and a cocktail of protease inhibitors). Lysates were boiled for 5 min and cleared by centrifugation. Protein concentrations were determined by a bicinchoninic acid protein assay (Sigma-Aldrich), and equal amounts of proteins were separated on 10% SDS-PAGE gels, immunoblotted with (phospho-)MLC2 or (phospho-)p42/44 MAPK antibodies and detected with an enhanced chemiluminescence system (Amersham, Piscataway, NJ). Bands representing (phospho-)MLC2 were quantified using Scion Image software.

Electron Microscopy

Transmission Electron Microscopy (TEM). Cells were washed several times with 6.8% saccharose to remove serum in 0.1 M cacodylate buffer, pH 7.4, at RT and then fixed for 30 min at RT in 2% glutaraldehyde in 0.1 M cacodylate buffer, pH 7.4. The cells were rinsed three times in the same buffer with 6.8% sucrose and subsequently postfixed in 2% OsO_4/3% $K_4Fe(CN)_6$ in 0.2 M cacodylate buffer, pH 7.4, at 4°C for 1 h. After rinsing in 0.1 M cacodylate buffer, pH 7.4, and dehydration in a graded alcohol series, the cells were embedded in Epon 812 and polymerized for 2 d at 58°C. Finally, ultrathin sections (60 nm) were cut and stained with uranyl acetate and lead citrate. The sections were examined using a Philips CM 100 electron microscope operating at 80 kV, and micrographs were taken.

Scanning Electron Microscopy. Coverslips with cells or after cell removal were fixed with 2% glutaraldehyde in 0.1 M cacodylate buffer, pH 7.4, and washed (0.2 M cacodylate buffer, pH 7.4, for 15 min and subsequently with distilled water for 10 min). Samples were then dehydrated with ethanol (30, 50, 70, 96, and 100% in steps of 10 min, followed by two times 30 min with 100% ethanol). Samples were subsequently dried with a Baltec CPD 030 critical point dryer, allowing ethanol to CO_2 exchange. Sample coating was done with Au/Pd ~3 nm (Sputtercoater Balzers 120B), and samples were analyzed using a JEOL JSM-6301F cold field emission scanning electron microscope operating at 2 kV and at 60 or 600× magnification.

Statistics

A two-tailed unpaired Student's t test (assuming equal variances) was used to assess whether the means of two data sets were statistically different. The assumption of normality for the performed t tests was verified with a Kolmogorov–Smirnov test.

RESULTS

Apical Lumen Formation in HepG2 Cells

Human hepatoma HepG2 cells (Knowles *et al*., 1980) provide a cell culture model system to study modulation of the liver phenotype that occurs during fetal/adult development or during liver regeneration (Kelly and Darlington, 1989), and they have been shown to be an excellent model for the study of apical plasma membrane biogenesis, i.e., cell polarity development (Bouma *et al*., 1989; Chiu *et al*., 1990; Sormunen *et al*., 1993; Zaal *et al*., 1994; Zegers *et al*., 1998; van IJzendoorn and Hoekstra, 1999). When cultured on glass coverslips, HepG2 cells acquire a polarized phenotype, demonstrated by the appearance of apical lumens (BC) between adjoining cells, in a time-dependent manner (Figure 2A). BC are readily visualized by the presence of apical resident proteins (Roelofsen *et al*., 2000; Aït Slimane *et al*., 2003) and by TRITC-phalloidin staining of the F-actin cytoskeleton, which is abundantly present underneath the apical surface (Figure 2D; Zegers and Hoekstra, 1998). Determination of the ratio BC/100 cells (as a measure for HepG2 cell polarity development; see *Materials and Methods*; cf. van IJzendoorn and Hoekstra, 1997, 1998; Zegers and Hoekstra, 1997) at 24, 48, and 72 h after plating reveals an initial steady increase in the number of apical lumens in time and a subsequent decrease after 48 h (Figure 2A). Approximately 25 BC/100 cells were counted in 48-h-old cell cultures, which decreased to 20 BC/100 cells in 72-h-old cell cultures (Figure 2A; cf. van IJzendoorn and Hoekstra, 1997, 1998). A representative image of a 72-h-old polarized HepG2 cell culture, showing TRITC-phalloidin–labeled BC and Hoechst-33528–stained nuclei, is depicted in Figure 2, C–E.

We next determined the number of cells that participated in a single BC as a function of time. For this, cells were fixed at the different time points and stained with TRITC-phalloidin and Hoechst-33528. TRITC-phalloidin–labeled BC were

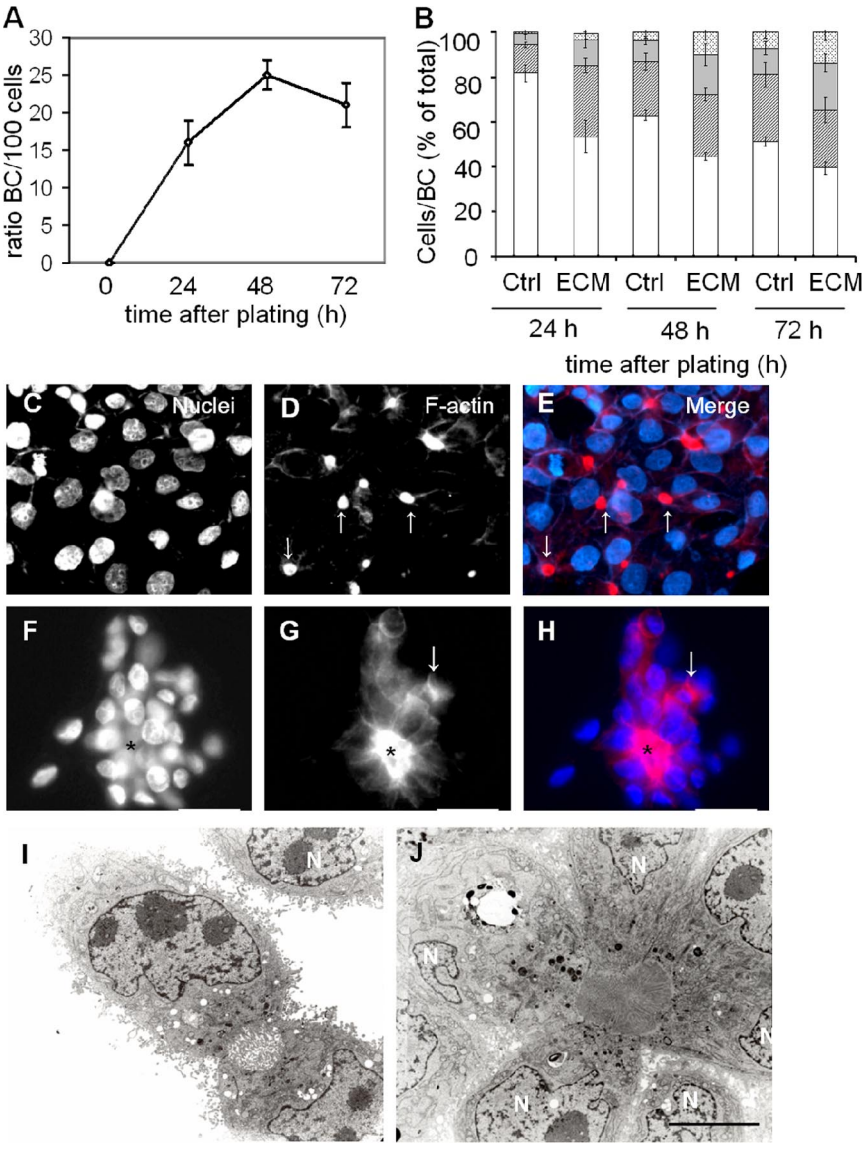

Figure 2. ECM affects apical lumen morphology in HepG2 cell cultures. (A) Apical polarity development in HepG2 cells as a function of time after plating, expressed as the ratio BC/100 cells. Data are expressed as mean ± SD of three independent experiments carried out in duplicate. (B) Average number of cells participating in a single BC (expressed as the ratio cells/BC) as a function of time after plating on glass coverslips (Ctrl) or predeposited ECM (ECM). Data are expressed as mean ± SD of three independent experiments carried out in duplicate. White, hatched, gray, and dotted bars represent BC shared by two, three, four, or more than five cells, respectively. Student's *t* tests to determine the statistical significance between Ctrl and ECM at 24 h: white bars, $p < 0.02$; hatched bars, $p < 0.003$; gray bars, $p = 0.11$; dotted bars, $p = 0.2$; at 48 h: white bars, $p < 0.003$; hatched bars, $p = 0.4$; gray bars, $p < 0.001$; dotted bars $p < 0.05$; at 72 h: white bars, $p < 0.01$; hatched bars, $p = 0.26$; gray bars, $p = 0.07$; dotted bars, $p < 0.05$. Student's *t* tests to determine the statistical significance of control cells between 24 and 48 h, $p < 0.05$; between 48 and 72 h, $p < 0.01$. (C–H) Polarized morphology of HepG2 cells plated on glass coverslips (C–E) or predeposited ECM (F–H). Hoechst-stained nucleus in C and F, TRITC-phalloidin stained BC in D and G, and merged pictures in E and H. Bars, 10 μm. (I and J) TEM image of polarized HepG2 cells plated on glass coverslips (I) or predeposited ECM (J). N, nucleus. Bar, 5 μm.

identified, and the number of cells associated with the BC was determined. Interestingly, the number of cells sharing a single BC (ratio cells/BC) increased in time. Thus, whereas 24 h after plating >80% of the BC were shared by two cells (couplets), 48–72 h after plating this percentage was reduced to 50–60%, whereas other BC were shared by three (~30% of all BC) or even more than five (~15% of all BC) cells (Figure 2B, Ctrl; $p < 0.05$). These data suggest that, in addition to the previously reported formation of apical lumens between two adjacent cells, subsequent apical lumen morphogenesis occurs in time to form larger lumens that span multiple cells.

HepG2 Cells Plated on Predeposited ECM Display Clustering, Cell Multilayering, and Remodeling of Apical Lumens

Because the number of HepG2 cells participating in a single apical lumen increased as a function of time (Figure 2B), which would be consistent with the deposition of increasing amounts of ECM by the cells, we next investigated the effect of ECM on apical lumen formation in HepG2 cells by culturing the cells on predeposited HepG2 ECM. To obtain coverslips coated with HepG2 ECM, HepG2 cells were first grown onto sterilized glass coverslips until confluence (3–5 d). Then, the cells were removed from the coverslips with distilled water, leaving deposited ECM on the coverslip (see *Materials and Methods* and Supplemental Figure S1). The ECM-coated coverslips were subsequently incubated with DMEM at 37°C and used for the culture of a new batch of cells. After different times of culturing, cells grown on predeposited ECM were fixed and double stained with TRITC-labeled phalloidin to visualize the apical lumens and Hoechst-33528 to visualize the nuclei. As shown in Figure 2, F–H, HepG2 cells displayed a dramatically altered spatial organization when cultured on predeposited HepG2 ECM. Thus, whereas on glass coverslips cells grow predominantly as a monolayer (Figure 2, C–E), on deposited ECM a reorganization of the cells is observed that includes cell clustering and cell multilayering (visualized by overlapping nuclei; see Figure 1, F versus C). The percentage of cells displaying multilayering was accurately estimated by the following equation: multilayering = $((\text{nuclei}_{\text{total}} - \text{nuclei}_{\text{single}})/\text{nuclei}_{\text{total}}) \times 100\%$, in which $\text{nuclei}_{\text{single}}$ refers to nuclei that

do not overlap in the x-z direction with other nuclei (see *Materials and Methods*). At least 10 fields per coverslips, each containing >50 cells, were analyzed. Whereas only 10 ± 3% of the cells cultured on glass coverslips displayed multilayering, 47 ± 6% of the cells cultured on predeposited ECM multilayered (p value from an unpaired *t* test = 0.03).

Most strikingly, culturing the cells on predeposited ECM induced the formation of large elongated apical lumens that span multiple cells, resembling the first clear indication of parenchymal organization in embryonic and regenerating liver (Ogawa *et al*., 1979; Stamatoglou *et al*., 1992). Indeed, whereas in control cells BC are typically located between two neighboring cells, in cells cultured on ECM, BC were predominantly shared by multiple, sometimes up to 10 cells (Figure 2, F–H, compare with C–E). The association of multiple cells with a single lumen in cells cultured on predeposited ECM was confirmed by TEM (Figure 2, I and J). When HepG2 cells were cultured on coverslips coated with only laminin, collagens, fibronectin, or the integrin nonspecific substrate poly-L-lysine, remodeling of apical lumens was not observed (our unpublished data). Furthermore, culturing the cells in low-serum (0.5% FCS) or serum-free medium did not change the outcome of the experiments (our unpublished data), suggesting that serum-derived factors may not be critical for ECM-mediated cell reorganization and apical lumen remodeling.

To add a quantitative measure to the ECM-mediated apical lumen remodeling, the number of cells that shared a single BC was determined as a function of time in cell cultures grown on glass coverslips or predeposited ECM. In Figure 2B, the percentage of BC shared by two cells (white bars), three cells (hatched bars), four cells (gray bars), or more than five cells (dotted bars) in cell cultures grown on glass coverslips (Ctrl) and predeposited ECM (ECM) is shown. Whereas in cultures plated on glass coverslips the percentage of BC shared by two cells was >80% at 24 h and gradually decreased to 50–60% at 72 h, in cultures grown on predeposited ECM for 24 h the percentage of BC shared by two cells was dramatically reduced to ~50% and continued to decrease to ~40% at 72 h. Most strikingly is the approximately twofold increase (from 15 to 30%; $p < 0.05$) in the percentage of BC shared by four or more than five cells in cultures grown for 72 h on predeposited ECM, compared with cells grown on glass coverslips (Figure 2B). Together, these data suggest that hepatocytes can modulate their own cell-to-cell organization and polarized morphology through the deposition of ECM.

ECM-mediated Apical Lumen Remodeling Does Not Perturb Apical Plasma Membrane Characteristics and Functioning

We next determined whether the membranes lining the remodeled apical lumens in ECM-grown cell cultures displayed typical apical plasma membrane characteristics. First, we verified that apical resident proteins such as MDR1 (Aït Slimane *et al*., 2003) and villin were exclusively localized to the BC (Figures 3, A–C. and 4, C and D, respectively). Moreover, apical plasma membrane-associated MDR1 readily translocated R123, a fluorescent substrate for MDR1, into the apical space (Figure 3, D–F), suggesting that the MDR1 protein was functioning properly. Importantly, no leakage of R123 into the basolateral space was observed, which suggests that the apical lumens are enclosed in between the cells and separated from the basolateral space by tight junctions. Indeed, the tight junction protein ZO-1 localized to the lumens (Figure 3, G–I) and morphologically distinguishable electron-dense apical junctions were readily observed at opposing membranes with transmission electron microscopy (Figure 3, J and K). Moreover, laser scanning confocal microscopy confirmed that the multicellular apical lumens, (immuno)labeled for the apical bile canalicular protein MRP2 and F-actin, were enclosed in the cell clusters (Supplementary Figure S2 and supplemental animated projections M1 and M2). As a final test to examine whether the tight junctions bordering the enclosed apical lumens displayed a proper "fence" function, cells were labeled with the fluorescent lipid analogue C_6-NBD-SM at 4°C, allowing incorporation of the probe in the outer leaflet of the plasma membrane. Nonincorporated lipid analogue was then removed by three wash steps at 4°C and the cells were examined with the fluorescence microscope. As shown in Figure 3L, C_6-NBD-SM labeled the basolateral surface but was not detected at the apical domain, indicating that the apical lumen is enclosed within the cells and separated from the basolateral space by functional tight junctions. In another experiment, cells were incubated with C_6-NBD-SM at 37°C for 30 min, allowing transcytosis of the lipid probe to the BC (van IJzendoorn *et al*., 1997; van IJzendoorn and Hoekstra, 1998). Then, C_6-NBD-SM remaining at the basolateral surface was removed with BSA at 4°C (see *Materials and Methods*). Cells were subsequently incubated at 4°C for 30 min and examined. As shown in Figure 3M, C_6-NBD-SM remained localized predominantly at the BC, and no significant diffusion of the probe to the basolateral domain was observed, indicating a proper fence function of the tight junctions. Together, these data suggest that cells cultured on predeposited ECM for 72 h display typical characteristics and functioning of the canalicular plasma membrane.

Inhibition of Rho Kinase (ROCK) Mimics ECM-mediated Cell Reorganization and Apical Lumen Remodeling

The small GTPase Rho and its downstream effector Rho kinase (ROCK) have recently been implicated in the regulation of polarized epithelial cell architecture (Sahai and Marshall, 2002; Vaezi *et al*., 2002; Omelchenko *et al*., 2003; Wozniak *et al*., 2003; Eisen *et al*., 2004; Prahalad *et al*., 2004), presumably by interpreting extracellular signals such as those provided by the ECM. To investigate the possible involvement of ROCK in the ECM-mediated HepG2 cell remodeling, cells were first cultured on glass coverslips in the absence or presence of the specific ROCK inhibitor Y-27632 (2.5 μM). In the absence of the ROCK inhibitor, HepG2 cells formed a monolayer and developed BC in between two or three cells (Figure 4, A and B; cf. Figure 2, C–E). In striking contrast, inhibition of ROCK induced clustering and multilayering (>10-fold compared with nontreated cells) of the cells and induced remodeling of the apical lumen, similarly as observed in cells cultured on predeposited ECM (Figure 4, C and D; compare with Figure 2, F–H). Determination of the percentage of BC shared by two, three, four, or more than five cells showed a more than twofold increase in the number of BC shared by four or more than five cells (Figure 4E, gray and dotted bars, respectively), whereas the percentage of BC shared by two or three cells (Figure 4E, white and hatched bars) was reduced from >80% in control cells to ~50% in Y-27632–treated cells. The large apical lumens in ROCK-inhibited cells were lined with a dense F-actin network (Figure 4, K and M) and contained the microvilli protein villin (Figure 4D). The integrity of the apical plasma membrane was unperturbed, verified similarly as described for cells cultured on predeposited ECM (our unpublished data; cf. Figure 3 and Supplemental Figure S2).

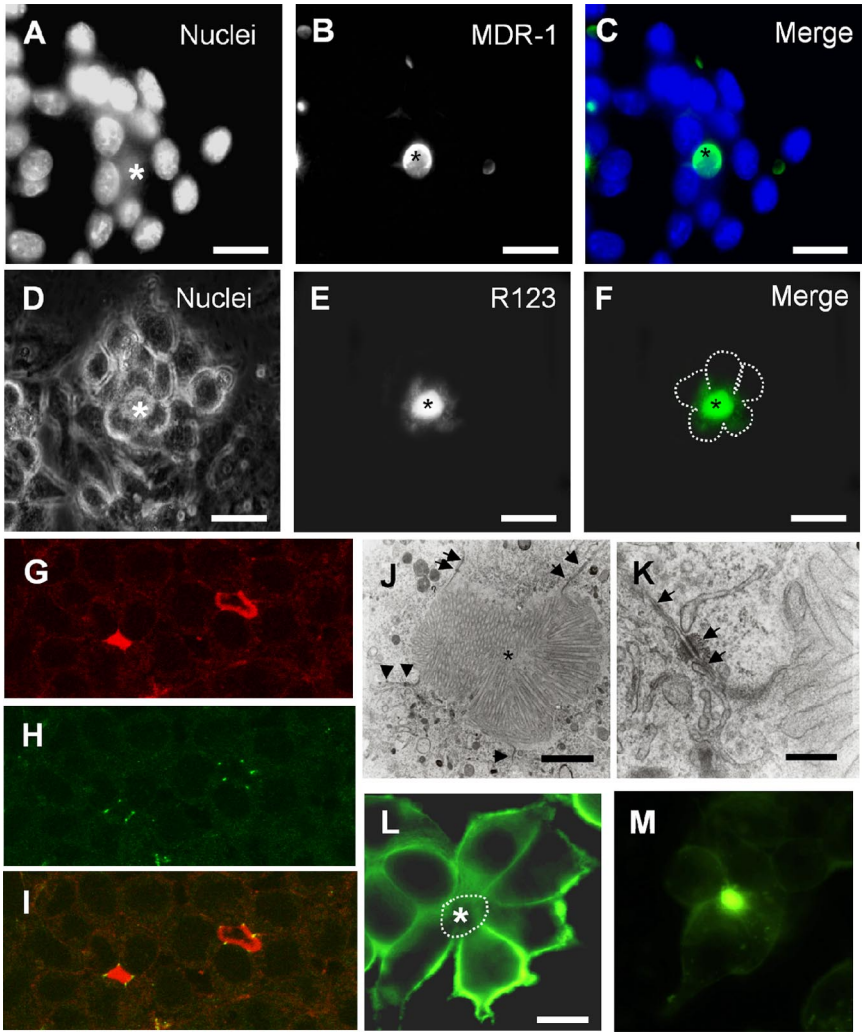

Figure 3. ECM-remodeled lumens display apical membrane identity. (A–C) Apical lumens in cells cultured for 3 d on predeposited ECM present the canalicular transporter MDR1 (A, nuclei; B, MDR1; and C, merged image). (D–F) The MDR1 substrate R123 is translocated and contained in the apical lumen of cells cultured on predeposited ECM for 3 d (D, phase contrast; E, R123; and F, merged image). (G–I) Tight junction protein ZO-1 (H) borders the apical domain, visualized with TRITC-phalloidin (G). Merged image in I. (J and K) TEM image of the apical lumen (J, black asterisk) and apical junctions (K, arrows) of cells (indicated with white asterisks in J) cultured on predeposited ECM. (L) C6-NBD-SM at the basolateral surface does not diffuse to the apical membrane (asterisk) of cells cultured on predeposited ECM. (M) C6-NBD-SM in the apical plasma membrane domain of cells cultured on predeposited ECM does not diffuse to the basolateral domain. Bars in A-I, L, and M, 10 μm. Bars in J and K, 2 μm and 100 nm, respectively.

Multicellular apical lumens may form de novo and/or develop at the expense of existing individual BC. To investigate this, we cultured cells on glass coverslips for 2 d in normal cell culture medium, and, subsequently, for another 24, 48, or 72 h in the presence of Y-27632. After 2 d in culture, apical lumens were predominantly observed between two or three cells (Figure 4, F and G, arrows; cf. Figure 2, C–E). After a subsequent 24-h culture in the presence of Y-27632, cells had clustered and in the cell clusters multiple larger apical lumens could be observed (Figure 4, H and I). After another 24 h in the presence of Y-27632, cell multilayering became apparent and larger multicellular apical lumens were typically observed in cell clusters, often with other smaller apical lumens present in the same cell cluster (Figure 4, J and K, arrows). The smaller apical lumens disappeared in time, leaving a single large and often elongated multicellular apical lumen (Figure 4, L and M). Along with this apparent transition of small lumens in between 2 cells to larger multicellular lumens, the absolute number of apical lumens in Y-27632–treated cell cultures decreased in time (Figure 4N). Not only Y-27632–treated cells but also nontreated cells plated on glass coverslips for up to 96 h continued to develop larger multicellular lumens (>4 or 5 cells/lumen; $p < 0.05$) with a concomitant decrease in the number of small lumens in between two or three cells (Figure 5A; $p < 0.05$), and with a concomitant decrease in the total number of lumens in the culture (Figure 5B). Moreover, laser scanning confocal microscopy and subsequent three-dimensional reconstruction of apical lumens in HepG2 cells cultured on predeposited ECM for 72 h revealed noticeable coalescence of apical lumens (Figure 5, C–E, and Supplementary Movie Clip M3). Together, these data suggest that HepG2 cells can abandon their monolayer phenotype to form clusters of multilayered cells and that large multicellular apical lumens can develop concomitant with a decrease in the number of preexisting individual BC, possibly as a result of their merging. Importantly, cell clustering and apical lumen remodeling is significantly increased upon culturing of the cells on predeposited ECM or upon the inhibition of Rho kinase.

ETA Metabolism-stimulated ROCK Activity Prevents ECM-mediated Cell Reorganization and Apical Lumen Remodeling

The virtually identical morphological effects of Y-27632 compared with the effects of predeposited ECM strongly suggest that inhibition of ROCK represents a key factor in the ECM-mediated cell reorganization and apical lumen remodeling. To investigate this, we treated cells cultured on predeposited ECM with ETA (50 μM), known to stimulate Rho signaling and ROCK activity (Feng *et al*., 1999; Araki *et al*., 2001). Indeed, the formation of stress fibers at the basal

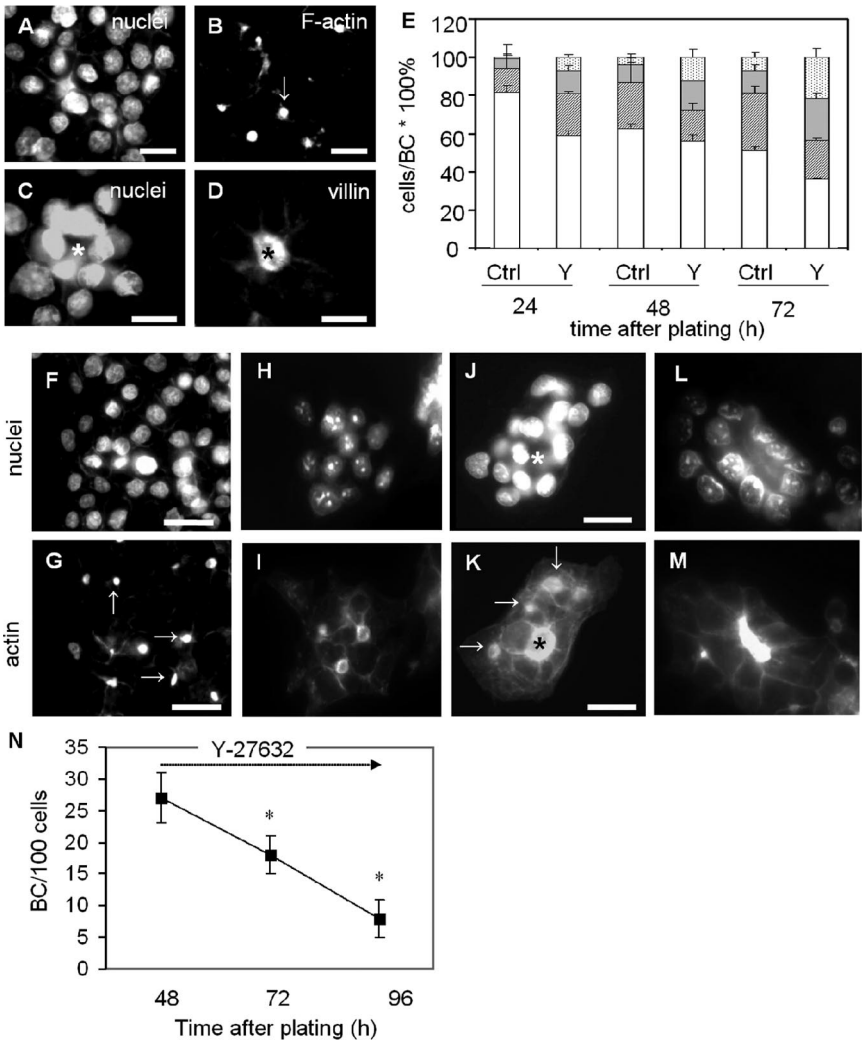

Figure 4. Involvement of ROCK activity in apical lumen morphogenesis. (A–D) Inhibition of ROCK in cells cultured on glass coverslips with Y-27632 for 3 d induces apical lumen remodeling (C and D), compared with nontreated cells (A and B). A and C, DAPI-stained nuclei; B, TRITC-phalloidin–labeled BC; D, villin-labeled BC. (E) Average number of cells that participate in a single BC of control (Ctrl) or Y-27632–treated (Y) cells as a function of time after plating. White, hatched, gray, and dotted bars represent BC shared by two, three, four, or more than five cells, respectively. Student's *t* tests: 24 h: Ctrl versus Y-27632, white bars, $p < 0.001$; hatched bars, $p < 0.004$; gray bars, $p < 0.02$; dotted bars, $p = 0.2$; 48 h: Ctrl versus Y-27632, white bars, $p < 0.01$; hatched bars, $p < 0.02$; gray bars, $p < 0.004$; dotted bars $p < 0.01$; and 72 h: Ctrl versus Y-27632, white bars, $p < 0.001$; hatched bars, $p < 0.05$; gray bars, $p < 0.01$; dotted bars, $p < 0.005$. (F–M) Cells were cultured for 48 h and treated with Y-27632 for 0 h (F and G), 24 h (H and I), 48 h (J and K), or 72 h (L and M). Cells were fixed and labeled with DAPI to visualize the nuclei (F, H, J, and L) and TRITC-phalloidin to visualize the BC lumens (G, I, K, and M). Bars, 10 μm. (N) Cells were cultured for 48 h and treated with Y-27632 for 0, 24, or 48 h. Cells were fixed and labeled with DAPI and TRITC-phalloidin to calculate the ratio BC/100 cells. Data are expressed as mean ± SD of three independent experiments carried out in duplicate. *$p < 0.05$.

surface of HepG2 cells (our unpublished data), and a Y-27632–sensitive increase in the phosphorylation status of the well-known ROCK target myosin light chain-2 (MLC2) at serine-19 (Totsukawa *et al.*, 2000; Figure 7A), confirmed that ETA stimulates ROCK activity. The addition of ETA in the cell culture medium completely blocked the ECM-mediated cell reorganization and apical lumen remodeling (Figure 6B, compare with A). Thus, whereas cell reorganization and apical lumen remodeling was apparent in cultures grown on predeposited ECM (Figure 6A), treatment with ETA resulted in monolayer cell cultures with small apical lumens in between two or three cells (Figure 6B), indistinguishable from control cells grown on glass coverslips (cf. Figure 2, C–E). Indeed, determination of the percentage of BC shared by two cells (white bars), three cells (hatched bars), four cells (gray bars), or more than five cells (dotted bars) in ETA-treated cultures showed a complete block of the effects of predeposited ECM and no significant differences compared with cells grown on glass coverslips (Figure 6E). Interestingly, the inhibitory effect of ETA was rescued when cells were cotreated with the lipoxygenase inhibitor NDGA (10 μM; Figure 6, C and E), which blocks the conversion of ETA to leukotrienes, the latter of which have been reported to mediate the ETA-stimulated Rho signaling (Setoguchi *et al.*, 2001; Thodeti *et al.*, 2002; Roberts *et al.*, 2003). Together, these data strongly suggest that ECM induces cell reorganization and apical lumen remodeling by down-regulating ROCK activity. In addition, lipoxygenase-controlled ETA metabolism antagonizes ECM-mediated cell reorganization. Importantly, treatment of the cells with ETA did not inhibit apical lumen formation per se (Figure 6B), suggesting that the development of apical lumens between adjacent cells and the subsequent remodeling of apical lumens to form multicellular canals are controlled by distinct signaling pathways.

We next investigated whether cell clustering, multilayering, and apical lumen remodeling required a continuous down-regulation of ROCK activity. For this, cells were cultured on predeposited HepG2 ECM for 72 h to allow the morphological response as described in Figures 2 and 3, after which the cells were treated for another 24 h in the presence of ETA to stimulate ROCK activity. Control cells were cultured for 24 h in the absence of ETA. As shown in Figure 6D, the ECM-mediated morphological changes could not be reversed by ETA. However, it was readily observed that the apical lumens displayed a more constricted morphology compared with cells that had not been treated with ETA (Figure 6D; cf. A). These data suggest that the ECM-mediated and ROCK down-regulation-mediated effects on cell clustering, multilayering, and apical lumen remodeling do not require continuous down-regulation of ROCK activity, and, in addition, suggest that ROCK activity is actively involved in regulating contraction and shape of the multicellular apical lumens.

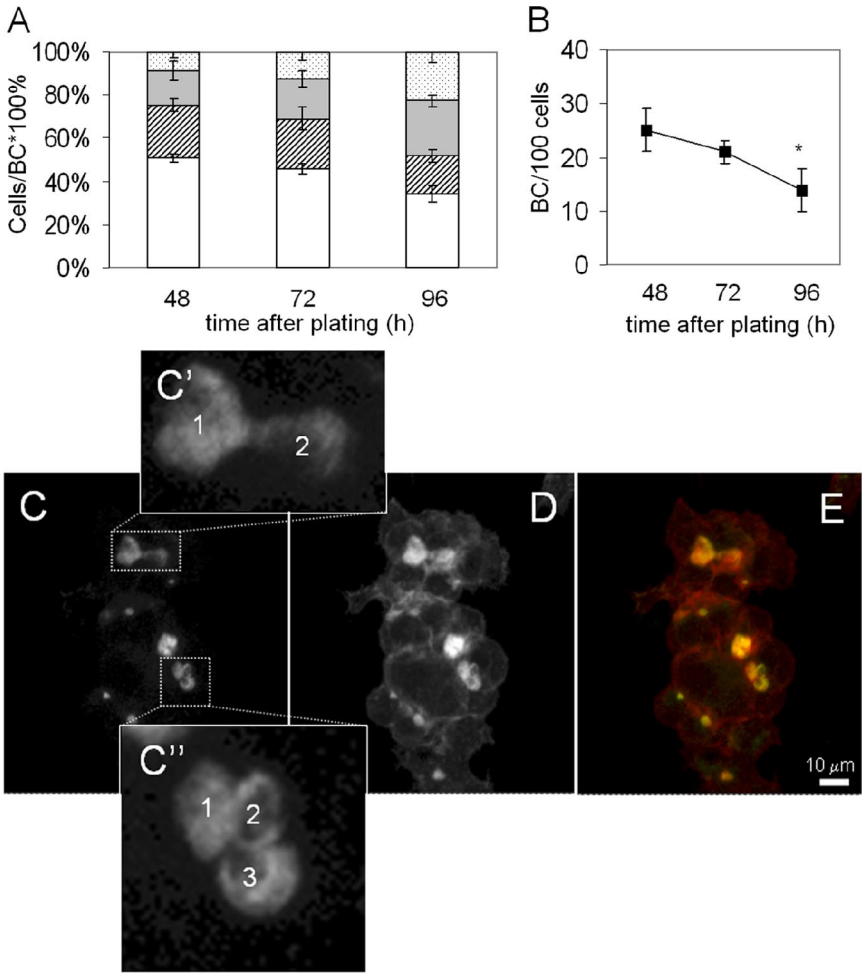

Figure 5. Apical lumen remodeling in cells cultured on glass coverslips for >48 h. Cells were cultured on glass coverslips for 48 h and subsequently for another 0, 24, or 48 h. Cells were then fixed, and the ratio cells/BC (A) and BC/100 cells (B) was determined as described in *Materials and Methods*. Data are expressed as mean ± SD of three independent experiments carried out in duplicate. *$p < 0.05$. (C–E) Cells cultured on glass coverslips for 72 h were fixed and (immuno)labeled with anti-MRP2 antibodies (C–C″) and TRITC-labeled phalloidin (D) and subjected to laser scanning confocal microscopical. Multiple x-y sections (1/0.5 μm) were superimposed. A merged image is shown in E. C′ and C″ are enlargements of the respective boxes in C, and the numbers indicate distinct apical lumens.

Inhibition of Myosin II ATPase Mimics the Effects of ECM or ROCK Inhibition on Cell Reorganization and Apical Lumen Remodeling

Membrane contraction, including the bile canalicular membrane (Tsukada *et al*., 1995), is typically controlled by actin–myosin interactions. MLC2 is a well-characterized downstream target of ROCK, and its phosphorylation at serine-19 results in increased actin–myosin-based contractility. In polarized HepG2 cells, MLC2 predominantly localizes to the apical domain of the cells (Figure 7C), revealing a pattern reminiscent of that observed for tight junction proteins (cf. van der Wouden *et al*., 2002). Phosphorylated MLC2 also

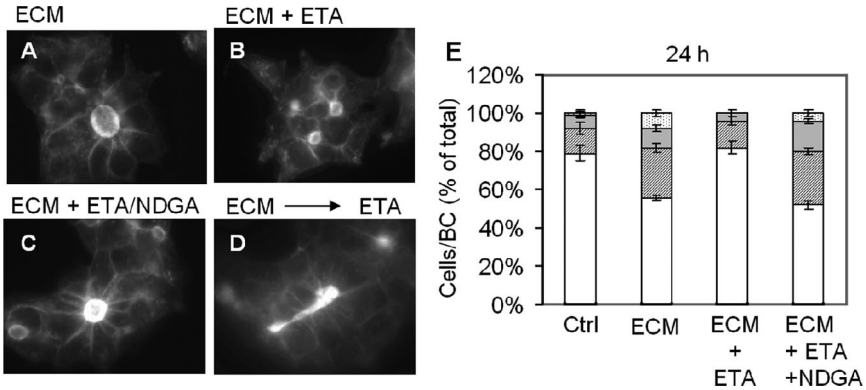

Figure 6. Effects of ETA metabolism on ECM-mediated apical lumen remodeling. (A) TRITC-phalloidin-labeled apical lumen in cells cultured on ECM for 3 d. (B) TRITC-phalloidin–labeled apical lumen in cells cultured on ECM for 3 d in the presence of ETA. (C) TRITC-phalloidin–labeled apical lumen in cells cultured on ECM for 3 d in the presence of ETA + NDGA. (D) TRITC-phalloidin–labeled apical lumen in cells cultured on ECM for 48 h, followed by treatment with Y-27632 for 24 h. Bar, 10 μm. (E) Average number of cells that participate in a single BC of HepG2 cells cultured on glass coverslips (Ctrl), ECM, ECM + ETA, or ECM + ETA + NDGA for 24 h. White, hatched, gray and dotted bars represent BC shared by two, three, four, or more than five cells, respectively. Student's *t* tests: white bars, Ctrl versus ECM, $p < 0.001$; ECM versus ECM + ETA, $p < 0.001$; ECM + ETA versus ECM + ETA + NDGA, $p < 0.001$; hatched bars, Ctrl versus ECM, $p = 0.006$; ECM versus ECM + ETA, $p = 0.44$; ECM + ETA versus ECM + ETA + NDGA, $p = 0.42$; gray bars, Ctrl versus ECM, $p = 0.90$; ECM versus ECM + ETA, $p = 0.14$; ECM + ETA versus ECM + ETA + NDGA, $p = 0.03$; and dotted bars, Ctrl versus ECM, $p = 0.008$; ECM versus ECM + ETA, $p = 0.014$; ECM + ETA versus ECM + ETA + NDGA, $p = 0.39$.

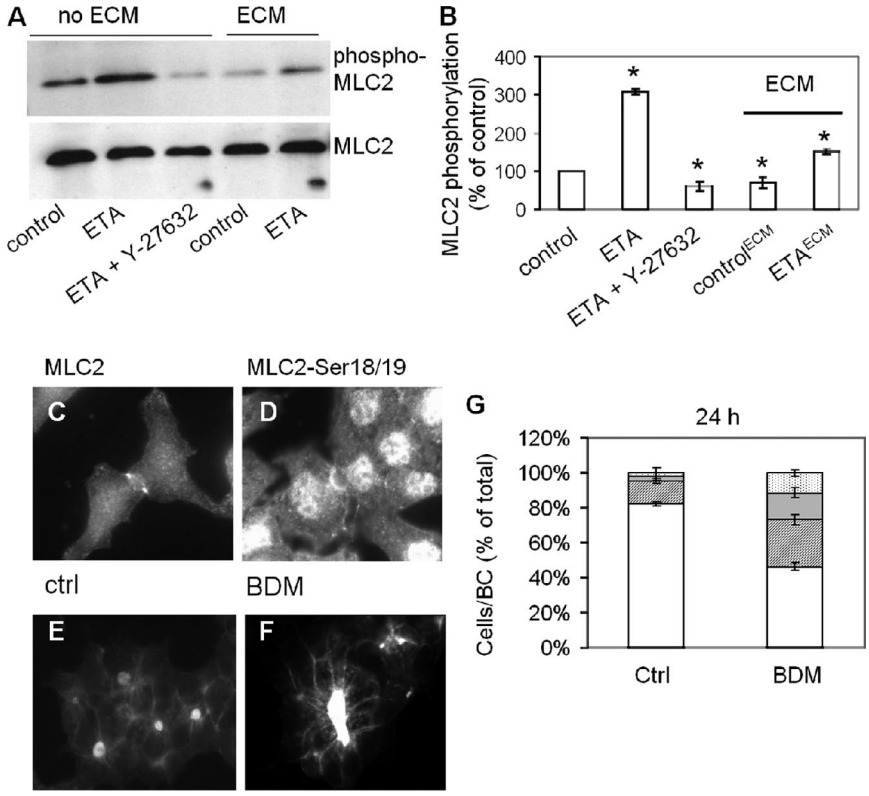

Figure 7. Involvement of myosin II in apical lumen remodeling. (A) Western blot showing expression level of phosphorylated MLC2 and total MLC2 in cells cultured on glass coverslips (no ECM) that were untreated or treated with ETA or ETA + Y-27632 for 24 h, and in cells cultured on predeposited ECM that were untreated or treated with ETA for 24 h. (B) The mean normalized alteration in MLC2 phosphorylation was calculated by quantification of electrophoretic bands of three experiments using Scion Image software, expressed as (phospho-MLC2/total MLC2) × 100%, and presented as percentage of control. *$p < 0.05$ in a Student's *t* test (ETA versus control, ETA + Y-27632 versus control, control^{ECM} versus control, ETA^{ECM} versus control^{ECM}). (C) MLC2 localizes to the tight junction area of HepG2 cells. (D) Phosphorylated MLC2 localizes to the tight junction area and nucleus of HepG2 cells. (E and F) Culturing HepG2 cells on glass coverslips in the presence of BDM for 24 h induces apical lumen remodeling (E), compared with nontreated cells (D). (F) The average number of cells that participate in a single BC in HepG2 cells cultured for 24 h in the presence or absence of BDM. White, hatched, gray, and dotted bars represent BC shared by two, three, four, or more than five cells, respectively. Student's *t* tests: white bars, Ctrl versus BDM, $p < 0.001$; hatched bars, Ctrl versus BDM, $p < 0.001$; gray bars, Ctrl versus BDM, $p = 0.001$; dotted bars, Ctrl versus BDM, $p = 0.002$.

localizes to the apical domain, and, in addition, was observed at the nucleus (Figure 7D). Treatment of the cells with 50 μM ETA, which inhibits ECM-mediated apical lumen remodeling, increases MLC2 phosphorylation in a Y-27632–sensitive manner (Figure 7, A and B), whereas culturing HepG2 cells on predeposited ECM results in a reduced level of phosphorylated MLC2 (Figure 7, A and B). These data suggest that the effects of ECM and ROCK inhibition on cellular reorganization and apical lumen remodeling may be due to a decrease in myosin function. To further investigate this, we examined whether inhibition of myosin ATPase activity could mimic the effects of ECM and ROCK inhibition. For this, cells were cultured on glass coverslips in the absence or presence of the myosin heavy chain ATPase inhibitor BDM (10 mM). As shown in Figure 7F, cells treated in the presence of BDM displayed similar cell clustering, multilayering, and apical lumen morphogenesis as observed in cells cultured on predeposited ECM (cf. Figure 2, F–H) or in the presence of 2.5 μM Y-27632 (cf. Figure 4, A–D). Determination of the percentage of BC shared by two, three, four, or more than five cells showed a more than 10-fold increase ($p = 0.001$) in the number of BC shared by four or more than five cells (Figure 7G, gray and dotted bars, respectively), whereas the percentage of BC shared by two or three cells (Figure 7G, white and hatched bars, respectively) was reduced from >80% in control cells to ~45% in Y-27632–treated cells ($p < 0.001$). The effects of BDM could not be counteracted by the addition of ETA to the culture medium (our unpublished data), suggesting that myosin-II ATPase acts downstream of ROCK. The effects of BDM on cell clustering and apical lumen remodeling could be reproduced with 100 μM blebbistatin, another inhibitor of myosin-II ATPase (Supplemental Figure S3). Together, these data strongly suggest that the effects of predeposited ECM and ROCK inhibition are, at least in part, mediated by the reduced phosphorylation status of MLC2 and consequent inhibition of myosin-II heavy chain ATPase activity.

Apical Lumen Morphogenesis but Not Cell Multilayering Requires p42/44 MAPK

MAPKs (p42/44 MAPK) can be activated upon extracellular cues and have been implicated in epithelial multilayering and apical morphogenesis (O'Brien *et al.*, 2004). To examine the role of p42/44 MAPK in the ECM-mediated cell clustering, multilayering, and apical lumen remodeling, cells were cultured on predeposited ECM for 72 h in the presence of 50 μM PD98059, a selective inhibitor of the mitogen-activated protein kinase kinase (MEK)-p42/44 MAPK signaling pathway. In the presence of PD98059, HepG2 cells cultured on predeposited ECM failed to undergo apical lumen remodeling (Figure 8, D–F) as observed in nontreated cells (Figure 8, A–C). Indeed, the ratio cells/BC in cells cultured on predeposited ECM in the presence of PD98059 was similar to that observed in control cultures grown on glass coverslips (Figure 8H). However, PD98059-treated cells did cluster and displayed cell multilayering on ECM to a similar extent compared with nontreated cells (Figure 8G). Similar data were obtained with another inhibitor of the MEK–MAPK signaling pathway, UO126 (10 μM; our unpublished data). These data suggest that p42/44 MAPK activity is required at a stage subsequent to cell multilayering but before apical lumen remodeling. We did not observe an alteration in the level of phosphorylated p42/44 MAPK in cells cultured on predeposited ECM or in the presence of Y-27632 (Figure 8I), suggesting that endogenous MAPK signaling may act as a dominant parallel signaling pathway.

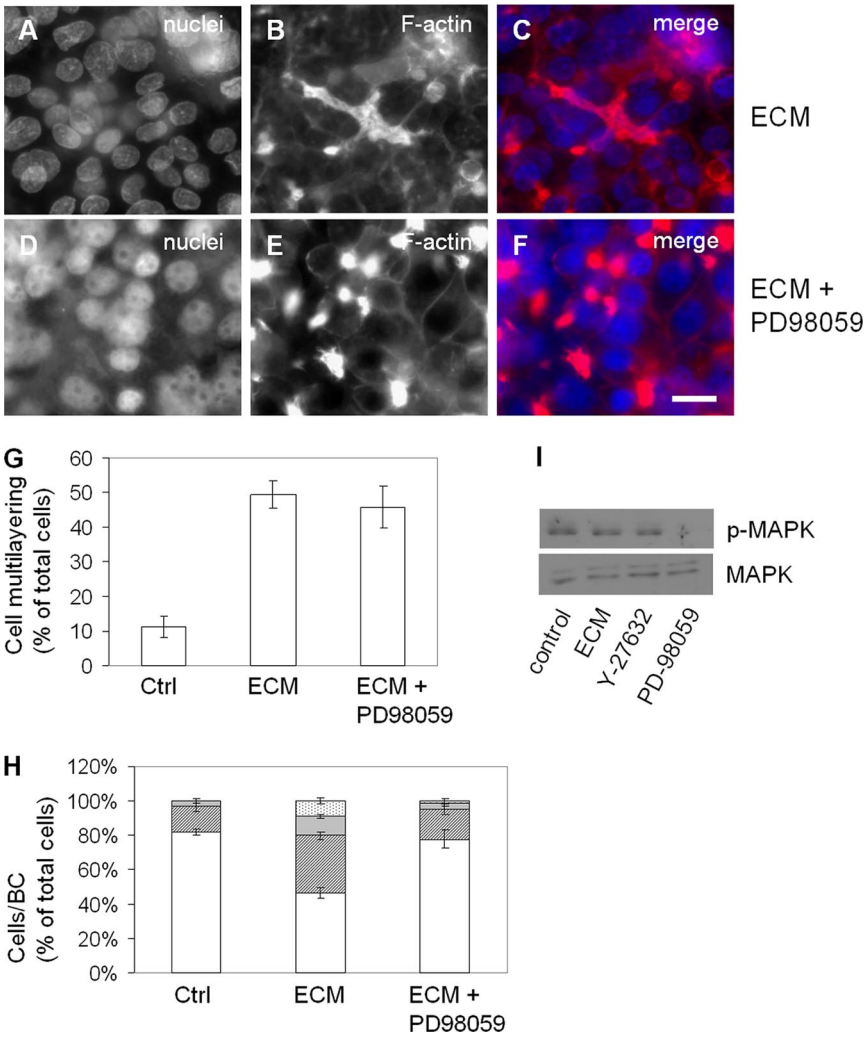

Figure 8. Apical lumen remodeling but not cell multilayering requires MAPK signaling. (A–C) Apical lumen remodeling in cells cultured on predeposited ECM for 72 h (A, nuclei; B, TRITC-phalloidin; and C, merged image). (D–F) Apical lumen remodeling in response to predeposited ECM is inhibited by PD98059 (D, nuclei; E, TRITC-phalloidin; and F, merged image). Bar, 10 μm. (G) Percentage of total cells that display multilayering (see *Materials and Methods*) when cultured on glass coverslips or on predeposited ECM for 72 h in the presence of absence of PD98059. Student's *t* test: Ctrl versus ECM, $p < 0.001$; Ctrl versus ECM + PD98059, $p = 0.001$; ECM versus ECM + PD98059, $p = 0.48$. (H) Average number of cells participating in a single BC in cell cultured on glass coverslips or on predeposited ECM for 72 h in the presence or absence of PD98059. White, hatched, gray, and dotted bars represent BC shared by two, three, four, or more than five cells, respectively. Student's *t* tests: white bars, Ctrl versus ECM, $p < 0.001$; ECM versus ECM + PD98059, $p < 0.001$; hatched bars, Ctrl versus ECM, $p < 0.001$; ECM versus ECM + PD98059, $p < 0.001$; gray bars, Ctrl versus ECM, $p < 0.001$; ECM versus ECM + PD98059, $p = 0.002$; dotted bars, Ctrl versus ECM, $p < 0.001$; ECM versus ECM + PD98059, $p < 0.001$. (I) Western blot showing expressing levels of p42/44 MAPK and phospho-MAPK in control cells, cells cultured on predeposited ECM for 72 h, or cells cultured in the presence of Y-27632 or PD-98059 for 72 h. Note the virtual absence of phosphorylated MAPK in PD98059-treated cells, whereas ECM and Y-27632 have no effect on the level of phosphorylated MAPK.

DISCUSSION

The molecular mechanisms and signaling cascades that contribute to the development and morphogenesis of apical lumens in hepatocytes and other epithelial cells are not well understood, but are clearly regulated by the extracellular environment, including adjacent cells and the ECM (Ojakian et al., 1997; Yeaman *et al*., 1999). When plated on glass coverslips, hepatoma HepG2 cells grow as a monolayer culture, and, in time, develop apical vacuoles in between two or three cells (Figure 2), consistent with previous reports (Bouma *et al*., 1989; Chiu *et al*., 1990; Sormunen *et al*., 1993; van IJzendoorn *et al*., 1997; Falasca *et al*., 1999; Ishigami *et al*., 2005). When plated on coverslips onto which ECM had previously been deposited by HepG2 cells, the spatial organization of the cells dramatically and rapidly changes, evidenced by the self-assembly of cells in multilayering cell clusters. In addition, apical lumens readily form larger, elongated structures that span multiple cells (Figures 2 and 3). The membranes delineating these multicellular lumens display proper apical bile canalicular plasma membrane characteristics with regard to protein composition and functionality, contain numerous microvilli and are physically separated from the basolateral space by adherens and tight junctions (Figure 3). The multicellular apical lumens closely resemble the first clear indication of parenchymal organization in embryonic and regenerating liver (Ogawa *et al*., 1979; Stamatoglou *et al*., 1992). In vivo, such cellular rearrangement occurs transiently during development and regeneration (preceding plate formation) but appears to be the end stage of morphological differentiation during carcinogenesis (Stamataglou *et al*., 1994). The formation of an elaborate, anastomosing canalicular network subsequent to the development of an acinar morphology was not apparent within the time span of our experiments, although some branching of the canalicular lumen was observed (Figure 8, B and C). Because the transition from small apical lumens between two cells to larger multicellular (>5 cells) lumens occurs concomitantly with a decrease in the total number of apical lumens in the culture, and because serial confocal microscopy x-y sections reveal the clustering of apical lumens during this process, it is tempting to speculate that the large multicellular apical lumens may form, at least in part, via the merging of existing BC (Figures 4, F–N, and 5). This process has been named "cord hollowing," where pockets of fluid-filled lumens occur at the lateral cell surfaces along the central axis of a multicellular cord, which then expand by virtue of ongoing delivery of apical vesicles, and, by an unknown mechanism, coalesce to form tubular structures (Lubarsky and Krasnov, 2003). The cord hollowing model is in agreement with the morphological stadia described in

early studies on bile canalicular development in rat livers in vivo (De Wolf-Peeters *et al*., 1974; Luzzatto, 1981; Kanamura *et al*., 1990) and in primary cocultures with rat small hepatocytes and nonparenchymal cells (Sudo *et al*., 2004). Together, our data suggest that hepatocyte-derived ECM may contribute to multicellular patterning and bile canalicular surface remodeling and offer an experimentally controlled hepatic model system in which bile canalicular lumen morphogenesis can be induced and the underlying molecular mechanisms studied.

The remodeling of apical lumens seems to be regulated by distinct signaling pathways, including lipoxygenase-controlled ETA metabolism, the small GTPase Rho effector protein ROCK, its downstream target myosin-II ATPase, and p42/44 MAPK activity. Indeed, cell patterning, i.e., the formation of multilayering cell clusters, and apical lumen remodeling in HepG2 cultures grown on predeposited ECM is completely inhibited upon addition of ETA in an NDGA-sensitive manner (Figure 6). ETA stimulates signaling by ROCK, evidenced by increased phosphorylation of MLC2 on serine-19 in a Y-27632–sensitive manner (Figure 7, A and B). Furthermore, the formation of multilayering cell clusters and remodeling of apical lumens can be induced in cell cultures grown on glass coverslips upon treatment of the cells with the specific ROCK inhibitor Y-27632 (Figure 4) or inhibitors of myosin-II heavy chain ATPase BDM and blebbistatin (Figure 7, F and G, and Supplemental Figure S3). Because the effects of myosin-II inhibition on cell reorganization and apical lumen remodeling could not be prevented with ETA, down-regulation of myosin-II ATPase activity likely occurs downstream of ROCK inhibition, consistent with MLC2 being a target for ROCK. The remarkably similar effects on cell–cell organization and apical lumen dynamics after culture on predeposited ECM or inhibition of ROCK/myosin-II suggest that the ECM down-regulates ROCK, and, subsequently, myosin-II ATPase activity, to stimulate cell patterning and apical lumen remodeling. Presumably, the uncoated glass coverslip precludes cell clustering and apical lumen remodeling by promoting high ROCK and myosin-II activity (Wozniak *et al*., 2003; Olson, 2004), which can be overcome by the deposition of sufficient amounts of ECM. Collagen-, laminin-, fibronectin-, or poly-L-lysine–coated coverslips failed to down-regulate MLC2 phosphorylation and did not induce the morphogenic effects as observed on predeposited ECM (our unpublished data), underscoring the necessity of correct signaling cascades initiated by the extracellular environment. The composition of the HepG2-derived ECM and the responsible integrins that link the extracellular ECM to the intracellular Rho signaling cascade remain to be investigated. Importantly, the inhibition or activation of ROCK and subsequent MLC2 phosphorylation does not visibly affect the formation of apical lumens per se (i.e., those formed between 2 or 3 cells), indicating that apical lumen formation and subsequent apical lumen remodeling are controlled by distinct mechanisms.

Although the involvement of the ROCK–myosin-II signaling cascade in HepG2 cell organization and apical lumen remodeling seems evident, the mechanism by which myosin-II ATPase contributes to this process remains elusive. The formation of extended canalicular lumens most likely requires lateral surface dynamics and apical junction remodeling (Zegers *et al*., 2003; Paul and Beitel, 2005), and myosin-II may play a role in regulating the dynamics of adhesion receptors (Bertet *et al*., 2004; Delanoe-Ayari *et al*., 2004; Shewan *et al*., 2005), consistent with its localization in HepG2 cells (Figure 7, C and D).

In addition to the involvement of ROCK and myosin-II, also p42/44 MAPK activity seems to be crucial for apical lumen remodeling, evidenced by the absence of canalicular lumen elongation in cell cultures grown on predeposited ECM in the presence of the specific MAPK signaling inhibitor PD98059 (Figure 8). Interestingly, in contrast to apical lumen remodeling, ECM-mediated cell multilayering was not affected by PD98059 treatment, suggesting that p42/44 MAPK signaling is involved in a step distal to that controlled by ROCK and myosin-II. We did not find evidence of ECM- or Y-27632–stimulated phosphorylation of p42/44 MAPK (Figure 8I), suggesting that basal MAPK activity is required.

Together, the data demonstrate that human HepG2 cells can be rapidly induced to adopt a organoid organization in an experimentally controlled manner and present lipoxygenase-controlled ETA metabolism, ROCK, myosin-II, and p42/44 MAPK as the first identified factors involved in hepatocyte-derived ECM-mediated multicellular patterning and bile canalicular lumen morphogenesis. Understanding the mechanisms that control this organoid organization and the consequent prospective to maintain liver-specific architecture and therewith correlated function of hepatocytes in culture is expected to advance the development of liver-related cell-based therapies, including the transplantation of (genetically modified) liver cells, the development of liver tissue substitutes for implantation, and/or toxicological screening, and extracorporeal circuits consisting of live cells.

ACKNOWLEDGMENTS

We thank Erik de Vries for expert technical assistance, Karin Klappe for preparing the C6-NBD-SM, and Ietse Stokroos for scanning electron microscopy. S.v.IJ. is supported by the Royal Dutch Academy of Sciences (KNAW).

REFERENCES

Abu-Absi, S. F., Friend, J. R., Hansen, L. K., and Hu, W. S. (2002). Structural polarity and functional bile canaliculi in rat hepatocyte spheroids. Exp. Cell Res. *274*, 56–67.

Aït Slimane, T., Trugnan, G., van IJzendoorn, S.C.D., and Hoekstra, D. (2003). Raft-mediated trafficking of apical resident proteins occurs in both direct and transcytotic pathways in polarized hepatic cells: role of distinct lipid microdomains. Mol. Biol. Cell *14*, 611–624.

Araki, S., Ito, M., Kureishi, Y., Feng, J., Machida, H., Isaka, N., Amano, M., Kaibuchi, K., Hartshorne, D. J., and Nakano, T. (2001). Arachidonic acid-induced Ca2+ sensitization of smooth muscle contraction through activation of Rho-kinase. Pflueg. Arch. Eur. J. Physiol. *441*, 596–603.

Bouma, M. E., Rogier, E., Verthier, N., Labarre, C., and Feldmann, G. (1989). Further cellular investigation of the human hepatoblastoma-derived cell line HepG 2, morphology and immunocytochemical studies of hepatic-secreted proteins. In Vitro Cell Dev. Biol. *25*, 267–275.

Bertet, C., Sulak, L., and Lecuit, T. (2004). Myosin-dependent junction remodelling controls planar cell intercalation and axis elongation. Nature *429*, 667–671.

Berthiaume, F., Moghe, P. V., Toner, M., and Yarmush, M. L. (1996). Effect of extracellular matrix topology on cell structure, function, and physiological responsiveness: hepatocytes cultured in a sandwich configuration. FASEB J. *10*, 1471–1484.

Chiu, J. H., Hu, C. P., Lui, W. Y., Lo, S. C., and Chang, C. M. (1990). The formation of bile canaliculi in human hepatoma cell lines. Hepatology *11*, 834–842.

Delanoe-Ayari, H., Al Kurdi, R., Vallade, M., Gulino-Debrac, D., and Riveline, D. (2004). Membrane and acto-myosin tension promote clustering of adhesion proteins. Proc. Natl. Acad. Sci. USA *101*, 2229–2234.

De Wolf-Peeters, C., De Vos, R., Desmet, V., Bianchi, L., and Rohr, H. P. (1974). Electron microscopy and morphometry of canalicular differentiation in fetal and neonatal rat liver. Exp. Mol. Pathol. *21*, 339–350.

DiPersio, C. M., Jackson, D. A., and Zaret, K. S. (1991). The extracellular matrix coordinately modulates liver transcription factors and hepatocyte morphology. Mol. Cell. Biol. *11*, 4405–4414.

Eisen, R., Ratcliffe, D. R., and Ojakian, G. K. (2004). Modulation of epithelial tubule formation by Rho kinase. Am. J. Physiol. *286*, C857–C866.

Feng, J., *et al*. (1999). Rho-associated kinase of chicken gizzard smooth muscle. J. Biol. Chem. *274*, 3744–3752.

Falasca, L., Marcellini, P., Ara, C., Rufo, A., and Devirgiliis, L. C. (1999). Growth inhibition and induction of specific hepatic phenotype expression by retinoic acid in HEPG2 cells. Anticancer Res. *19*, 3283–3292.

Feracci, H., Connolly, T. P., Margolis, R. N., and Hubbard, A. L. (1987). The establishment of hepatocyte cell surface polarity during fetal liver development. Dev. Biol. *123*, 73–84.

Friedman, S. L., Roll, F. J., Boyles, J., and Bissell, D. M. (1985). Hepatic lipocytes: the principal collagen-producing cells of normal rat liver. Proc. Natl. Acad. Sci. USA *82*, 8681–8685.

Gallin, W. J. (1997). Development and maintenance of bile canaliculi in vitro and in vivo. Microsc. Res. Tech. *39*, 406–412.

Hoekstra, D., Tyteca, D., and van IJzendoorn, S. C. (2004). The subapical compartment: a traffic center in membrane polarity development. J. Cell Sci. *117*, 2183–2192.

Ihrke, G., Neufeld, E. B., Meads, T., Shanks, M. R., Cassio, D., Laurent, M., Schroer, T. A., Pagano, R. E., and Hubbard, A. L. (1993). WIF-B cells: an in vitro model for studies of hepatocyte polarity. J. Cell Biol. *123*, 1761–1775.

Ishigami, A., Fujita, T., Inoue, H., Handa, S., Kubo, S., Kondo, Y., and Maruyama, N. (2005). Senescence marker protein-30 (SMP30) induces formation of microvilli and bile canaliculi in Hep G2 cells. Cell Tissue Res. *320*, 243–249.

Kanamura, S., Kanai, K., and Watanabe, J. (1990). Fine structure and function of hepatocytes during development. J. Electron Microsc. Tech. *14*, 92–105.

Kelly, J. H., and Darlington, G. J. (1989). Modulation of the liver specific phenotype in the human hepatoblastoma line Hep G2. In Vitro Cell Dev. Biol. *25*, 217–222.

Kinoshita, T., and Miyajima, A. (2002). Cytokine regulation of liver development. Biochim. Biophys. Acta *1592*, 303–312.

Knowles, B. B., Howe, C. C., and Aden, D. P. (1980). Human hepatocellular carcinoma cell lines secrete the major plasma proteins and hepatitis B surface antigen. Science *209*, 497–499.

Larkin, J. M., Woo, B., Balan, V., Marks, D. L., Oswald, B. J., LaRusso, N. F., and McNiven, M. A. (2000). Rab3D, a small GTP-binding protein implicated in regulated secretion, is associated with the transcytotic pathway in rat hepatocytes. Hepatology *32*, 348–356.

Lemaigre, F., and Zaret, K. S. (2004). Liver development update: new embryo models, cell lineage control, and morphogenesis. Curr. Opin. Genet. Dev. *14*, 582–590.

Lubarsky, B., and Krasnow, M. A. (2003). Tube morphogenesis: making and shaping biological tubes. Cell *112*, 19–28.

Luzzatto, A. C. (1981). Hepatocyte differentiation during early fetal development in the rat. Cell Tissue Res. *215*, 133–142.

Matsui, T., Kinoshita, T., Morikawa, Y., Tohya, K., Katsuki, M., Ito, Y., Kamiya, A., and Miyajima, A. (2002). K-Ras mediates cytokine-induced formation of E-cadherin-based adherens junctions during liver development. EMBO J. *21*, 1021–1030.

Moghe, P. V., Berthiaume, F., Ezzell, R. M., Toner, M., Tompkins, R. G., and Yarmush, M. L. (1996). Culture matrix configuration and composition in the maintenance of hepatocyte polarity and function. Biomaterials *17*, 373–385.

O'Brien, L. E., Tang, K., Kats, E. S., Schutz-Geschwender, A., Lipschutz, J. H., and Mostov, K. E. (2004). ERK and MMPs sequentially regulate distinct stages of epithelial tubule development. Dev. Cell. *7*, 21–32.

Ogawa, K., Medline, A., and Farber, E. (1979). Sequential analysis of hepatic carcinogenesis: a comparative study of the ultrastructure of preneoplastic, malignant, prenatal, postnatal, and regenerating liver. Lab. Investig. *41*, 22–35.

Ojakian, G. K., Nelson, W. J., and Beck, K. A. (1997). Mechanisms for de novo biogenesis of an apical membrane compartment in groups of simple epithelial cells surrounded by extracellular matrix. J. Cell Sci. *110*, 2781–2794.

Olson, M. F. (2004). Contraction reaction: mechanical regulation of Rho GTPase. Trends Cell Biol. *14*, 111–114.

Omelchenko, T., Vasiliev, J. M., Gelfand, I. M., Feder, H. H., and Bonder, E. M. (2003). Rho-dependent formation of epithelial "leader" cells during wound healing. Proc. Natl. Acad. Sci. USA *100*, 10788–10793.

Paul, S. M., and Beitel, G. J. (2005). Tubulogenesis: zipping up your fly. Curr. Biol. *15*, R70–R72.

Prahalad, P., Calvo, I., Waechter, H., Matthews, J. B., Zuk, A., and Matlin, K. S. (2004). Regulation of MDCK cell-substratum adhesion by RhoA and myosin light chain kinase after ATP depletion. Am. J. Physiol. *286*, C693–C707.

Roelofsen, H., Soroka, C. J., Keppler, D., and Boyer, J. L. (1998). Cyclic AMP stimulates sorting of the canalicular organic anion transporter (Mrp2/cMoat) to the apical domain in hepatocyte couplets. J. Cell Sci. *111*, 1137–1145.

Roelofsen, H., Wolters, H., Van Luyn, M. J., Miura, N., Kuipers, F., and Vonk, R. J. (2000). Copper-induced apical trafficking of ATP7B in polarized hepatoma cells provides a mechanism for biliary copper excretion. Gastroenterology. *119*, 782–793.

Roberts, L. A., Glenn, H., Hahn, C. S., and Jacobson, B. S. (2003). Cdc42 and RhoA are differentially regulated during arachidonate-mediated HeLa cell adhesion. J. Cell. Physiol. *196*, 196–205.

Sahai, E., and Marshall, C. J. (2002). ROCK and Dia have opposing effects on adherens junctions downstream of Rho. Nat. Cell Biol. *4*, 408–415.

Selden, C., Khalil, M., and Hodgson, H. (2000). Three dimensional culture upregulates extracellular matrix protein expression in human liver cell lines–a step towards mimicking the liver in vivo? Int. J. Artif. Organs *23*, 774–7781.

Senoo, H., Imai, K., Matano, Y., and Sato, M. (1998). Molecular mechanisms in the reversible regulation of morphology, proliferation and collagen metabolism in hepatic stellate cells by the three-dimensional structure of the extracellular matrix. J. Gastroenterol. Hepatol. *13* (suppl), S19–S32.

Setoguchi, H., Nishimura, J., Hirano, K., Takahashi, S., and Kanaide, H. (2001). Leukotriene C(4) enhances the contraction of porcine tracheal smooth muscle through the activation of Y-27632, a rho kinase inhibitor, sensitive pathway. Br. J. Pharmacol. *132*, 111–118.

Shewan, A. M., Maddugoda, M., Kraemer, A., Stehbens, S. J., Verma, S., Kovacs, E. M., and Yap, A. S. (2005). Myosin 2 is a key rho kinase target necessary for the local concentration of E-cadherin at cell-cell contacts. Mol. Biol. Cell *16*, 4531–4542.

Sormunen, R., Eskelinen, S., and Lehto, V. P. (1993). Bile canaliculus formation in cultured HEPG2 cells. Lab. Investig. *68*, 652–662.

Stamatoglou, S. C., Enrich, C., Manson, M. M., and Hughes, R. C. (1992). Temporal changes in the expression and distribution of adhesion molecules during liver development and regeneration. J. Cell Biol. *116*, 1507–1515.

Stamatoglou, S. C., and Hughes, R. C. (1994). Cell adhesion molecules in liver function and pattern formation. FASEB J. *8*, 420–427.

Sudo, R., Ikeda, S., Sugimoto, S., Harada, K., Hirata, K., Tanishita, K., Mochizuki, and Y., and Mitaka, T. (2004). Bile canalicular formation in hepatic organoid reconstructed by rat small hepatocytes and nonparenchymal cells. J. Cell Physiol. *199*, 252–261.

Thodeti, C. K., Massoumi, R., Bindslev, L., and Sjolander A. (2002). Leukotriene D4 induces association of active RhoA with phospholipase C-gamma1 in intestinal epithelial cells. Biochem. J. *365*, 157–163.

Tzanakakis, E. S., Hsiao, C. C., Matsushita, T., Remmel, R. P., and Hu, W. S. (2001). Probing enhanced cytochrome P450 2B1/2 activity in rat hepatocyte spheroids through confocal laser scanning microscopy. Cell Transplant. *10*, 329–342.

Totsukawa, G., Yamakita, Y., Yamashiro, S., Hartshorne, D. J., Sasaki, Y., and Matsumura, F. (2000). Distinct roles of ROCK (Rho-kinase) and MLCK in spatial regulation of MLC phosphorylation for assembly of stress fibers and focal adhesions in 3T3 fibroblasts. J. Cell Biol. *150*, 797–806.

Tsukada, N., Ackerley, C. A., and Phillips, M. J. (1995). The structure and organization of the bile canalicular cytoskeleton with special reference to actin and actin-binding proteins. Hepatology *21*, 1106–1113.

Vaezi, A., Bauer, C., Vasioukhin, V., and Fuchs, E. (2002). Actin cable dynamics and Rho/Rock orchestrate a polarized cytoskeletal architecture in the early steps of assembling a stratified epithelium. Dev. Cell *3*, 367–381.

van der Wouden, J. M., van IJzendoorn, S.C.D., and Hoekstra, D. (2002). Oncostatin M regulates membrane traffic and stimulates bile canalicular membrane biogenesis in HepG2 cells. EMBO J. *21*, 6409–6418.

van IJzendoorn, S.C.D., and Hoekstra, D. (1998). (Glyco)sphingolipids are sorted in sub-apical compartments in HepG2 cells: a role for non-Golgi-related intracellular sites in the polarized distribution of (glyco)sphingolipids. J. Cell Biol. *142*, 683–696.

van IJzendoorn, S.C.D., and Hoekstra, D. (1999). The subapical compartment: a novel sorting centre? Trends Cell Biol. *9*, 144–149.

van IJzendoorn, S.C.D., Theard, D., Van Der Wouden, J. M., Visser, W., Wojtal, K. A., and Hoekstra, D. (2004a). Oncostatin M-stimulated apical plasma membrane biogenesis requires p27(Kip1)-regulated cell cycle dynamics. Mol. Biol. Cell *15*, 4105–4114.

van IJzendoorn, S.C.D., Van Der Wouden, J. M., Liebisch, G., Schmitz, G., and Hoekstra, D. (2004b). Polarized membrane traffic and cell polarity development is dependent on dihydroceramide synthase-regulated sphinganine turnover. Mol. Biol. Cell *15*, 4115–4124.

van IJzendoorn, S.C.D., Zegers, M. M., Kok, J. W., and Hoekstra, D. (1997). Segregation of glucosylceramide and sphingomyelin occurs in the apical to basolateral transcytotic route in HepG2 cells. J. Cell Biol. *137*, 347–357.

Wakabayashi, Y., Dutt, P., Lippincott-Schwartz, J., and Arias, I. M. (2005). Rab11a and myosin Vb are required for bile canalicular formation in WIF-B9 cells. Proc. Natl. Acad. Sci. USA *102*, 15087–91502.

Wang, L., and Boyer, J. L. (2004). The maintenance and generation of membrane polarity in hepatocytes. Hepatology *39*, 892–899.

Wozniak, M. A., Desai, R., Solski, P. A., Der, C. J., and Keely, P. J. (2003). ROCK-generated contractility regulates breast epithelial cell differentiation in response to the physical properties of a three-dimensional collagen matrix. J. Cell Biol. *163*, 583–595.

Yeaman, C., Grindstaff, K. K., and Nelson, W. J. (1999). New perspectives on mechanisms involved in generating epithelial cell polarity. Physiol. Rev. *79*, 73–98.

Zaal, K. J., Kok, J. W., Sormunen, R., Eskelinen, S., and Hoekstra, D. (1994). Intracellular sites involved in the biogenesis of bile canaliculi in hepatic cells. Eur. J. Cell Biol. *63*, 10–19.

Zegers, M. M., and Hoekstra, D. (1997). Sphingolipid transport to the apical plasma membrane domain in human hepatoma cells is controlled by protein kinase C and PKA activity: a correlation with cell polarity in HepG2 cells. J. Cell Biol. *138*, 307–321.

Zegers, M. M., and Hoekstra, D. (1998). Mechanisms and functional features of polarized membrane traffic in epithelial and hepatic cells. Biochem. J. *336*, 257–269.

Zegers, M. M., O'Brien, L. E., Yu, W., Datta, A., and Mostov, K. E. (2003). Epithelial polarity and tubulogenesis in vitro. Trends Cell Biol. *13*, 169–176.

Zegers, M. M., Zaal, K. J., van IJzendoorn, S. C., Klappe, K., and Hoekstra, D. (1998). Actin filaments and microtubules are involved in different membrane traffic pathways that transport sphingolipids to the apical surface of polarized HepG2 cells. Mol. Biol. Cell *9*, 1939–1949.

Zhao, R., and Duncan, S. A. (2005). Embryonic development of the liver. Hepatology. *41*, 956–967.